

## Photometry of Saturated Stars in CCD Images

J. Maíz-Apellániz<sup>1</sup>

Space Telescope Science Institute, Baltimore, MD 21218, USA

**Abstract.** We describe here a simple general method to correct for the effects of saturation in CCD observations of point sources where the A/D saturation level is significantly lower than the pixel full-well capacity. The method is intended to complement the results from a PSF-fitting or aperture photometry package and is somehow different from the one developed by Gilliland (1994) for WFPC2 data. The current implementation has been tested with WFPC2 and STIS CCD data, yields uncertainties between 0.02 and 0.10 magnitudes, and can be easily adapted to other *HST* or non-*HST* imaging CCDs.

### 1. Introduction

The accuracy of bright-star photometry derived from CCD observations is limited by the A/D saturation level, the electron capacity of the pixel well, and the possible onset of non-linearity at high count levels (see, e.g. Howell 2000). The four WFPC2 chips and the STIS CCD are known to be highly linear below the A/D saturation level (Dolphin 2000b, Gilliland et al. 1999). Furthermore, the similarity between the full-well capacity and the A/D saturation level for the GAIN = 4 setting of the STIS CCD allows the detector to behave in a linear fashion even beyond saturation (Gilliland et al. 1999), since charge is simply transferred to neighboring pixels (a phenomenon known as bleeding). The behavior for the GAIN = 1 setting of the STIS CCD or for the WFPC2 chips is rather different, given that the full-well capacity is between one-and-a-half and four times the A/D saturation level, leading to a possible substantial loss of counts in the data.

### 2. Description of the method

We can distinguish two different types of saturated point sources: weak, where no pixel reaches its full-well capacity, and strong, where at least one does and bleeding occurs. Weakly saturated stars retain an approximate circular symmetry while strongly saturated ones are elongated since bleeding takes place preferentially in the vertical direction (Fig. 1). Given their pixel sizes and PSFs, the transition between the two regimes is expected to take place for the GAIN = 7 setting of the WFPC2 and the GAIN = 1 of the STIS CCD somewhere in between 4 and 7 total saturated pixels (for a single star).

Our method consists of selecting ten or more unsaturated stars in the same chip where the saturated stars are observed and using them as a reference to correct for the information lost due to saturation. Aperture photometry is performed on the unsaturated stars blocking the central pixels in a manner which simulates what would happen if the stars were brighter and saturated. Thus, for each star we obtain its real magnitude and the magnitudes we would obtain if any number of pixels between 1 and  $N_{\max}$  were saturated and the central pixels were not used for the calculation. Three choices can be used for the blocked central region: no bleeding affects adjacent non-saturated pixels, so only saturated ones are excluded (appropriate for the weak case); bleeding possibly affects

---

<sup>1</sup>ESA Space Telescope Division

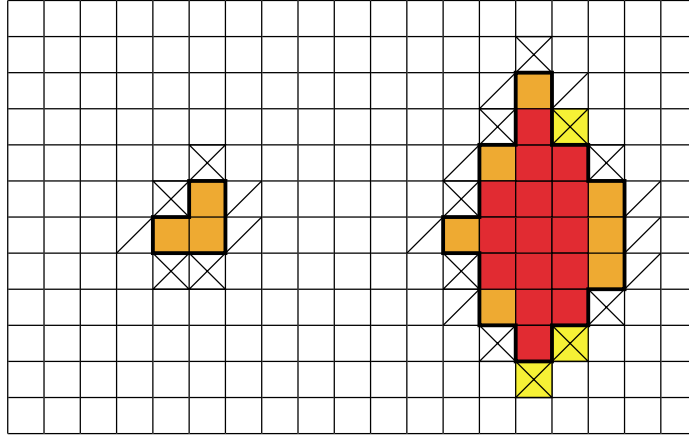


Figure 1. Examples of weakly (left) and strongly (right) saturated stars representative of WFPC2 (GAIN = 7) or STIS CCD (GAIN = 1) observations. The darkest shade is used to indicate pixels that have reached the full-well capacity, the intermediate one for those that are saturated but not completely filled, and the lightest one for not-saturated pixels that have suffered bleeding from pixels immediately below or above (only vertical bleeding is assumed here). The pixels possibly affected by vertical bleeding are marked with a cross and those possibly affected by horizontal (but not vertical) bleeding are marked with a diagonal line.

vertically adjacent pixels, so those are also excluded; and bleeding possibly affects both vertically and horizontally adjacent pixels, extending the exclusion to them (see Fig. 1). The magnitude differences for the reference stars are grouped by number of blocked pixels and within each group also by analogous geometrical kernels in order to account for the differences in pixel centering. For each kernel a mean magnitude correction and its dispersion is then calculated. The chip is then scanned for saturated stars, the pixels to be blocked are identified in each case, aperture photometry without the blocked pixels is performed, and the correction corresponding to that geometrical kernel is applied. Further corrections (CTE, geometrical distortions, aperture corrections) can easily be included.

This method has been implemented in an IDL code which currently handles up to  $N_{\max} = 6$  and the first two choices for blocked pixels. The other cases will be included in future versions. The advantages of this method are that no previous knowledge of the PSF or accurate calibration of the detector (in the form of e.g. some filter-dependent parameterization) are needed. Its main disadvantage is that the results will not be accurate if used for non-point sources.

### 3. Results

In order to test the accuracy of the method, we selected archival observations for which both short (unsaturated) and long (saturated) exposures of the same field existed. For WFPC2 (GAIN = 7), we used the F555W and F814W 30 Doradus data from program 5114 (P.I.: Westphal) and for STIS (GAIN = 1) the 50CCD NGC 6752 data from program 8415 (P.I.: Gilliland). The reference unsaturated photometry was obtained using HSTphot (Dolphin 2000a) for WFPC2 and a custom-made aperture photometry IDL code for STIS. We applied the method to the stars that had between 1 and 6 saturated pixels in the long exposure data. For WFPC2, only the PC and WF2 were tested and the stars in R136 were excluded due to the heavy crowding there. The two blocking options (weak and strong saturation) were tested. Results for the first one are shown in Figs. 2, 3, and 4 in terms of  $\Delta m$ , the difference between the magnitudes derived from the unsaturated and the saturated data.

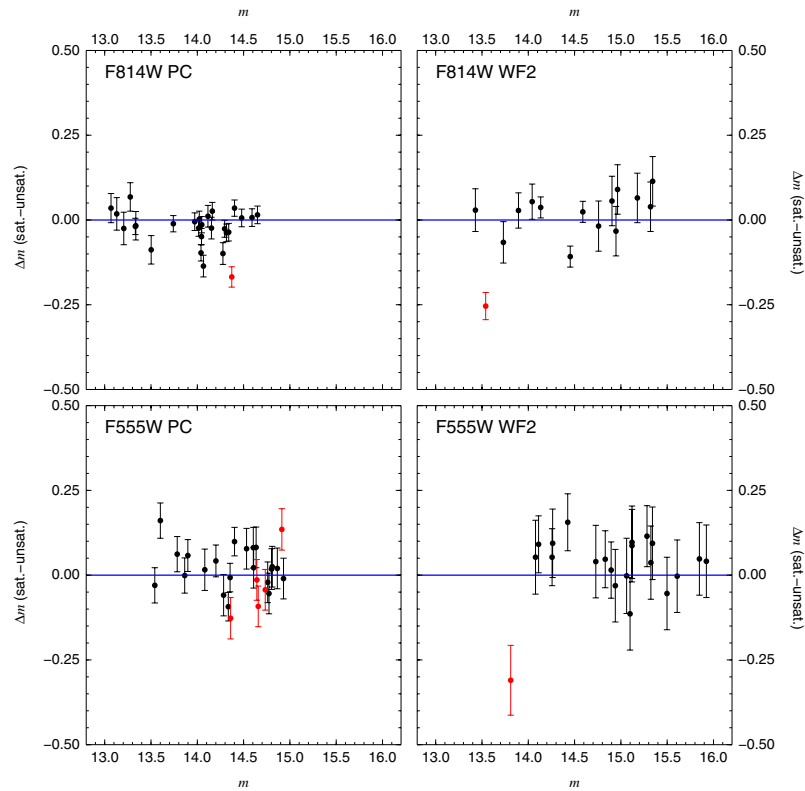


Figure 2. Measured magnitude difference between the saturated and unsaturated exposures as a function of magnitude for the weakly saturated stars in the WFPC2 observations of 30 Doradus. The saturated magnitudes were obtained using the method described in this poster while the unsaturated ones were obtained with HSTphot. Stars shown in gray are those with large values of  $\chi^2$  in HSTphot.

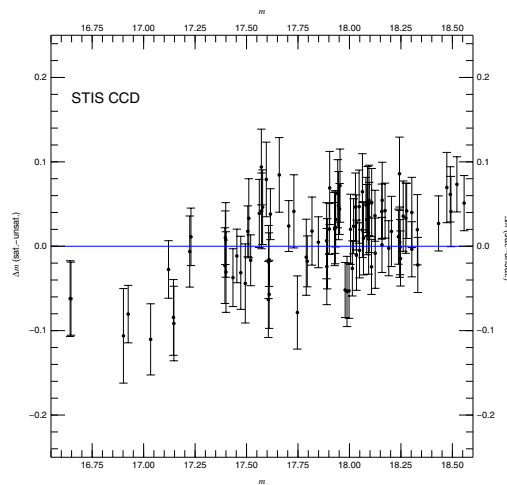


Figure 3. Same as Fig. 2 for the STIS CCD observations of NGC 6752. Here the unsaturated magnitudes were obtained by aperture photometry.

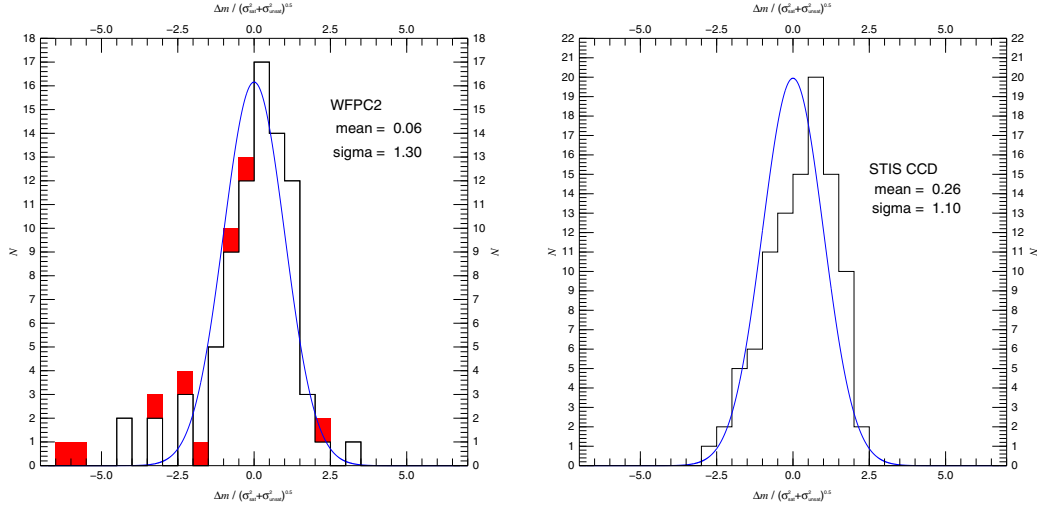


Figure 4. Measured magnitude difference normalized by its uncertainty for the WFPC2 (left) and STIS (right) results. The continuous curve shows the expected distribution. Gray blocks identify the gray data points in Fig. 2.

- The weak-saturation blocking option yields photometric uncertainties of 0.02–0.06 (PC), 0.05–0.10 (WF2), and 0.02–0.04 (STIS) magnitudes.
- The systematic bias generated by the algorithm is very small, of the order of 0.01 magnitudes for STIS and even smaller for WFPC2. In both cases the bias is also small in comparison with the measured uncertainty.
- No significant differences were found between the weak- and strong-saturation blocking options. Furthermore, no tendency in  $\Delta m$  as a function of  $m$  is observed in Fig. 2 and only a slight one is observed in Fig. 3. Therefore, the transition between the two modes of saturation appears to take place around  $N = 5$ – $6$  pixels for the STIS CCD and possibly at higher values for the WFPC2 chips.
- The distribution of  $\Delta m / (\sigma_{\text{sat}}^2 + \sigma_{\text{unsat}}^2)$  closely resembles a normal distribution (the limit  $N \rightarrow \infty$  of a Student's  $t$  distribution) for both the WFPC2 and STIS results. The only small divergences are the existence of a small bias in the STIS case and the presence of an extended left wing in the distribution for both cases. The latter phenomenon could be caused by the presence of stars with strong saturation or near-resolved binaries. This last interpretation is favored by the location of the stars with high values of  $\chi^2$  in the HSTphot output in Figs. 2 and 4.

## References

- Dolphin, A. E. 2000a, *PASP*, 112, 1383  
 Dolphin, A. E. 2000b, *PASP*, 112, 1397  
 Gilliland, R. L. 1994, *ApJ*, 435, L63  
 Gilliland, R. L., Goudfrooij, P., & Kimble, R. A. 1999, *PASP*, 111, 1009  
 Howell, S. B. 2000, *Handbook of CCD Astronomy*, CUP